Frog-Inspired Jumping Robot

Dihan Liu
Department of Mechanical and Aerospace Engineering
University of California San Diego
La Jolla, California

Kaiyu Liu
Department of Mechanical and Aerospace Engineering
University of California San Diego
La Jolla, California

***Abstract*—Over the years, significant progress has been made in the field of legged jumping robots, inspired by the dexterous movement patterns that organisms have evolved over millions of years. By applying the principles of bionics, engineers are trying to replicate the agile and adaptive movements of frogs into robot designs. These robots are particularly beneficial for tasks that span obstacles, work in hazardous environments, or in low-gravity conditions such as space, where they can navigate autonomously using their mobility. Frogs are excellent models for this work because of their strong land jumping abilities and underwater swimming skills, and despite their complex biological structure, they are of great study value. The challenge is to design robots that can effectively mimic these functions, which has led to a split in research focus between frog-inspired jumping robots and swimming robots. Our team's project is interested in frog-inspired jumping robots, and we plan to build a more in-depth dynamic model and discuss its jumping process. In this study, a simplified robot mechanism model is constructed. The model of non-slipping is derived. And the position, velocity and acceleration equations of the robot in the jumping stage are derived by using the D-H method. Then, based on the Lagrange method of multi-rigid-body dynamics, we formulate the dynamic equation of the robot in the take-off stage. Numerical solutions to the Lagrange equation are obtained through MATLAB.**

***Index Terms*—bio-inspired robot, frog, jumping**

I. Introduction

Valuable movement patterns for robots can be gleaned from observing animals in the natural world. Animal locomotion is a multifaceted and adaptable process that can be categorized into three main types: terrestrial movement, flight, and swimming. Among these, terrestrial locomotion stands out for its complexity and adaptability due to the varied and competitive environments it entails [1]. This mode of movement encompasses a range of actions such as walking, running, jumping, climbing, and crawling [2]. Jumping, in particular, offers distinct advantages in negotiating diverse and unpredictable terrains, surmounting obstacles, and swiftly evading threats. It demands quick bursts of energy and is often complemented by other locomotion methods like walking, gliding, or flapping. While some animals, such as kangaroos, primarily rely on jumping for movement, others like locusts utilize it to initiate flight [3].

Jumping enables animals, both vertebrates and invertebrates, to overcome obstacles much larger than their own size, facilitating rapid movements crucial for predator evasion and capturing elusive prey. Jumping animals employ various strategies based on their body structures and locomotion capabilities [4], [5]: 1. Continuous jumping, seen in animals like kangaroos, involves energy accumulation and continuous posture adjustment during both take-off and landing phases. 2. Intermittent jumping is utilized by smaller animals such as frogs, who need to reaccumulate energy after each landing.

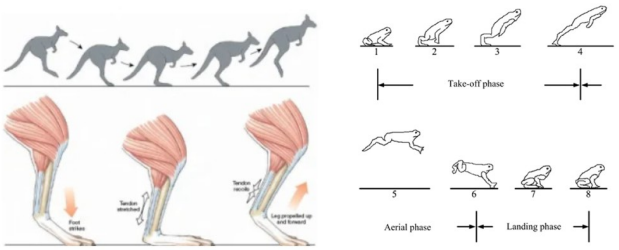

Fig. 1. Jumping of kangaroo and frog [6]

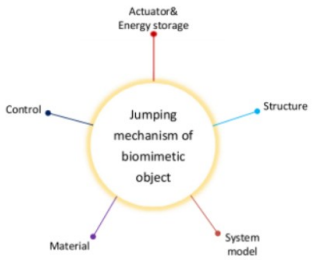

Fig. 2. Jumping mechanism of biomimetic object [8]

The remarkable jumping abilities of animals have inspired engineers to create robots that mimic them. They are particularly suitable for tasks in uneven, rough terrain such as battlefield reconnaissance, archaeological exploration, antiterrorism operations, freight transportation, patient care, and disaster relief [7]. Additionally, jumping robots show promise for interstellar exploration, as their ability to jump provides advantages in low-gravity environments like Mars and the moon. However, short jump cycles and instant bursts of power challenge. Mechanically complex jumping robots with multiple degrees of freedom and actuators are difficult to realize because of the complexity of control. Therefore, there is a focus on exploring efficient jumping mechanisms and driving modes to achieve small, minimally driven, intermittent and bionic jumping robots.

II. Background

In most jumping robot designs, electric motors are used to control energy storage and release through speed regulation. The most popular method of energy storage is elastic devices, and another common method of actuators and energy storage is the use of pneumatic devices. In addition to the above two, there are currently elastic materials and explosive gas (mixed hydrogen - oxygen gas) drive.

The advantages of pneumatic transmission are good compliance, large driving force, powerful general power, and strong dynamics. *Mowgli* is a typical pneumatically driven jumping robot (Fig 3 (a)). Its leg structure adopts the bionic design principle and is composed of 6 McKibben pneumatic muscle actuators. The maximum jumping height is about 0.5m, which exceeds 50% of the body height [9]. Driven by pneumatics, the robot can achieve stable jumps.

Springs offer significant advantages in terms of robust energy storage, rapid energy release, straightforward structure, and easy control, making them a prevalent choice in the design of biomimetic jumping robots. As far back as the 1880s, NASA devised a jumping robot inspired by the jumping mechanics of frogs. To address issues of low efficiency and excessive holding force, a design incorporating a 6-bar gear mechanism combined with a spring was developed (Fig 3 (b)). The linear spring, along with the six-bar gear mechanism, functions akin to a nonlinear spring [10].

As advancements in materials science continue, novel materials are being incorporated into biomimetic jumping robots, resulting in lighter weight and simpler structures. For instance, researchers have designed a biomimetic jumping kangaroo robot featuring semi-circular legs (Fig 3 (c)). These legs are crafted from fiberglass, which emulates the function of tendons in kangaroos [11].

By leveraging the benefits of novel materials such as elasticity, lightweight, and softness, in conjunction with the explosive properties of chemical gas, jumping robots can attain heightened energy density and explosive force to propel their movements, thereby enhancing their overall performance. As illustrated in Figure 3 (d), the chemical detonation can cause deformation within the soft body cavity, resulting in outward forces that perform work [12].

III. Proposed Work

Frogs, as quintessential amphibians, possess remarkable amphibious mobility. Their adeptness in navigating diverse natural terrains stems from the coordinated synergy of various movement modes, facilitating efficient and adaptable locomotion. Central to this capability is the explosive propulsion generated by their hind limbs, characterized by unified movement and control [13]. This tightly integrated motion pattern not only broadens the motion capabilities of robots but also enhances their mobility and stability through intermittent amphibious movements.

The high-output power and rapid response are required for frogs' intermittent swimming movements. Pneumatic artificial muscles, characterized by a high power-to-mass ratio and

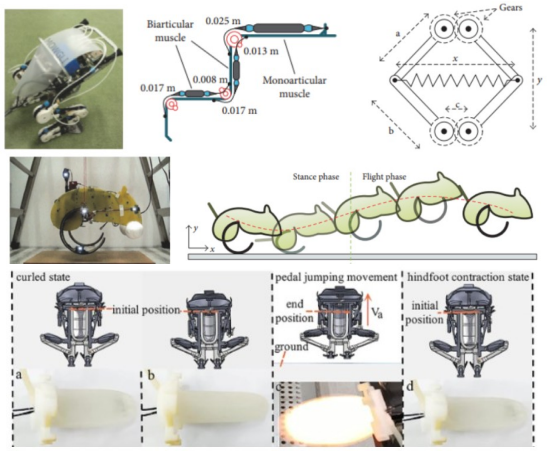

Fig. 3. (a) Mowgli developed by Tokyo Uni. [9] (b) NASA designed [10] (c) Jumping kangaroo using new material [11] (d) soft body detonation actuator [12]

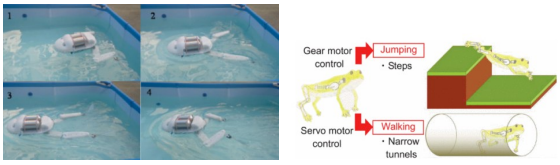

Fig. 4. Swimming and jumping-walking frog robot [14], [15]

flexibility akin to biological muscles, are well-suited for this purpose. Figure 5 illustrates a prototype utilizing pneumatic muscles as joint actuators to emulate frog swimming, incorporating three degrees of freedom in its legs. This prototype can swim autonomously, supported by integrated pneumatic, control, and communication systems within its body. Experimental and simulation results confirm the feasibility of driving the robot using pneumatic muscles, with the flow rate being the primary determinant of the pneumatic system's swift response [14].

Jumping robots commonly face challenges in adapting to abrupt terrain changes due to the absence of a flexible walking mode within their structure. While efficient jumping is typically achieved through mechanical systems, current research has not successfully addressed two key issues: (1) the ability to execute instantaneous jumps to surmount obstacles unsuitable for walking, and (2) precise control of leg joints for stable walking across rough terrain within a single compact body [15].

In addition to developing a frog robot that combines the above functions, how a frog jumps from the water is still a challenging task. The surface of the frog's own skin is moist, which helps them to move around in an environment with water. Researchers are exploring innovative materials and surface coatings to replicate the fluid dynamics of frog skin, allowing bionic frog robots to operate efficiently in aquatic environments.

In terms of perception and exploration, the combination of smart sensors and AI-driven algorithms can significantly

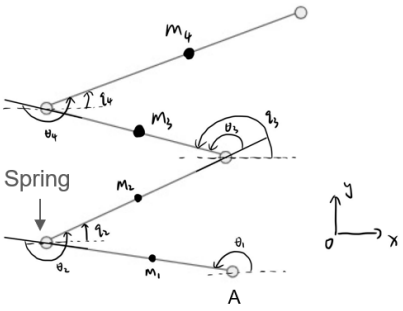

Fig. 5. Change of joint angle during take off

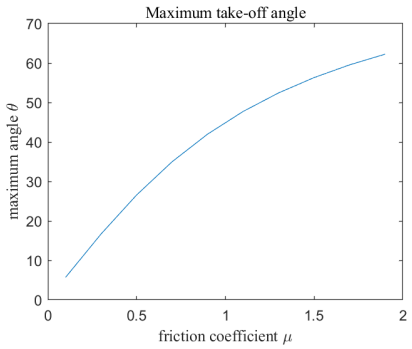

Fig. 6. Simulation of maximum take-off angle

enhance the frog robot's ability to perceive and interact with its environment. By combining advanced perception technologies such as cameras, lidar, and environmental sensors, coupled with sophisticated artificial intelligence algorithms for decision-making and navigation, frog-inspired robots are able to navigate and explore a variety of terrain in an agile and efficient manner, reflecting the superior adaptability of amphibious robots.

IV. Preliminary Work

Our research work focuses on the take-off scenarios of jumping robots. This section will present the conditions for robot take-off, as well as the derivation of the kinematic and dynamic models. In the part about take-off conditions, the project also investigates whether the robot might slip.

The model of the robot we built is a four-bar linkage as shown in Fig.5. In the initial stage of the robot's jumping process, the leg springs are in a compressed state, storing elastic potential energy. The robot is regarded as a system composed of rigid bodies connected by springs. The rigid body A is simplified to a point mass m, and $D-H$ represents the total energy of the system, which is the sum of potential energy and kinetic energy. The leg spring O has a natural length l_0, and when it is compressed to length l, it stores potential energy m_j, with j denoting the leg index $(j = 1, 2, 3, 4)$. The center of mass of each leg is at l_c, the angle each leg makes with the vertical is θ_j, and the position of the robot's center of mass is q_i, which varies over time. The spring to drive the robot is added on joint 2.

A. No slipping take off angle

The model of the robot before take-off is shown in the figure. Before take-off, the robot's palm is in full contact with the ground, hence there is a force F_{fl}, the floor reaction force, between the robot and the ground. The forces analyzed on the robot's palm include F_g, the gravity force, and F_{ak}, the force acting on the first ankle. There is also a torque τ_{ak} on the joint. l_{ak} represents the position vectors from the center of gravity to the ankle, and a represents the acceleration of the robot.

First, as gravity is present, the vertical component of F_{fl} is positive to provide support and friction to prevent slipping.

$$F_{fl\_y} >= 0 \tag{1}$$

By simulating the no-slipping model with column friction. We have friction f,

$$f = \mu * F_{fl\_y} \tag{2}$$

When the horizontal force of floor reaction force is smaller than friction, the robot will not slip.

$$F_{fl\_x} >= \mu * F_{fl\_y} \tag{3}$$

$$1/\mu > tan(\theta) \tag{4}$$

We can get the plot of the maximum take-off angle as shown in Fig.6. As the friction coefficient increases, the maximum takeoff angle also becomes larger. When the friction coefficient grows to a certain extent, the slope of the graph will decrease, indicating that there is no need to select an excessively high friction coefficient, as it does not significantly aid in increasing the maximum takeoff angle.

In the vertical direction, the direction of acceleration is upright

$$F_{fl\_y} - G - F_{ak} > 0 \tag{5}$$

And we get,

$$sin(\theta) > \frac{G + F_{ak}}{F_{fl}} \tag{6}$$

which is the restriction of the minimum angle. Assume the robot jumps with no twist, the torque balance is,

$$l_{ak} \times F_{ak} + \tau_{ak} + l_{fl} \times F_{fl} = 0 \tag{7}$$

and we can get the value of F_{fl}. Let l = 30 mm, h = 5 mm, m = 1 kg F_{ak} = 0-10 N and τ_{ak} = 2 N · m. The geometric relationships in the model are, $l_{ak} = \frac{1}{2}l, l_{fl} = \frac{1}{2}h$. The minimum take-off angle is shown in Fig.7. As the force of the ankle increases the minimum take-off angle decreases, which means the robot can take off nearly horizontally and can land at a further position.

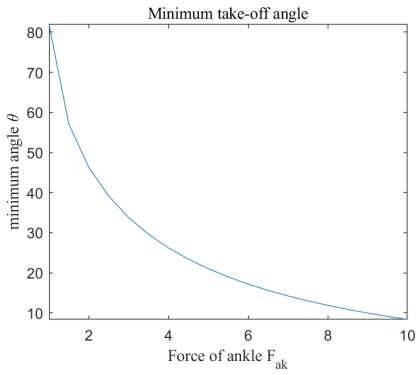

Fig. 7. Simulation of minimum take-off angle

B. Take off Kinematics and dynamics of the whole robot

For the four-bar linkages robot, the relationship of q_i and θ_i is given by the equations:

$$\begin{aligned} q_1 &= \theta_1, \\ q_2 &= \theta_1 + \theta_2, \\ q_3 &= \theta_1 + \theta_2 + \theta_3, \\ q_4 &= \theta_1 + \theta_2 + \theta_3 + \theta_4. \end{aligned}$$

The orientation matrix G_{α_i} is defined as:

$$G_{\alpha_i} = \begin{bmatrix} \cos q_i & -\sin q_i \\ \sin q_i & \cos q_i \end{bmatrix} \tag{8}$$

The position of each robot leg's center of mass in the global frame, denoted as $\mathbf{r}_c$, is essential for analyzing the robot's dynamic behavior and is given by:

$$\mathbf{r}_c = \begin{bmatrix} r_{c_1}, r_{c_2}, r_{c_3}, r_{c_4} \end{bmatrix} \tag{9}$$

Where:

$$\begin{aligned} \mathbf{r}_{c_1} &= \mathbf{r}_A + G_{\alpha_1}\mathbf{r}'_{c_1} = \begin{bmatrix} l_A + l_{c_1}\cos q_1 \\ l_{c_1}\sin q_1 \end{bmatrix}, \\ \mathbf{r}_{c_2} &= \mathbf{r}_B + G_{\alpha_2}\mathbf{r}'_{c_2} = \begin{bmatrix} l_A + l_{c_1}\cos q_1 + l_{c_2}\cos q_2 \\ l_{c_1}\sin q_1 + l_{c_2}\sin q_2 \end{bmatrix}, \\ \mathbf{r}_{c_3} &= \mathbf{r}_C + G_{\alpha_3}\mathbf{r}'_{c_3} = \begin{bmatrix} l_A + \sum_{i=1}^{3} l_{c_i}\cos q_i \\ \sum_{i=1}^{3} l_{c_i}\sin q_i \end{bmatrix}, \\ \mathbf{r}_{c_4} &= \mathbf{r}_D + G_{\alpha_4}\mathbf{r}'_{c_4} = \begin{bmatrix} l_A + \sum_{i=1}^{4} l_{c_i}\cos q_i \\ \sum_{i=1}^{4} l_{c_i}\sin q_i \end{bmatrix}. \end{aligned}$$

Here, $\mathbf{r}_A, \mathbf{r}_B, \mathbf{r}_C, \mathbf{r}_D$ represent the positions of the joints which connect the respective legs to the robot's body. The centroid of the robot, with the total mass denoted as m, and the local frame centroid as r_i, is given by:

$$r_{\text{com}} = \frac{1}{m}\sum_{i=1}^{4}(m_i r_i) \tag{10}$$

The global frame centroid is expressed as:

$$r_{\text{com}} = r_A + G(q)P \tag{11}$$

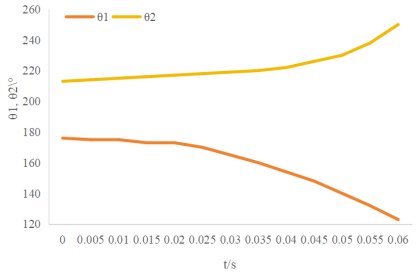

Fig. 8. Change of joint angle during take off

Where:

$$\begin{aligned} G(q) &= \begin{bmatrix} G_{\alpha_1} & G_{\alpha_2} & G_{\alpha_3} & G_{\alpha_4} \end{bmatrix}, \\ P &= \begin{bmatrix} P_1 & P_2 & P_3 & P_4 \end{bmatrix}^{\mathrm{T}} \end{aligned}$$

Furthermore, P_i represents the weighted average position of mass for example, $P_1 = \frac{m_1}{m}r_{c_1} + \frac{m_2+m_3+m_4}{m}r_B$. The acceleration of the robot is $\dot{r}_{\text{com}} == J(q)\dot{q}, and J(q) = \dot{G}(q)\dot{P}$.

The equations of motion for the system are obtained by applying the Lagrangian dynamics principle, which can be written as:

$$\frac{d}{dt}\frac{\partial L}{\partial \dot{q}_i} - \frac{\partial L}{\partial q_i} = \tau_i \tag{12}$$

Where $L(q,\dot{q}) = K(q,\dot{q}) - V(q)$, and τ_i is 0 in this model because no torque is added to the robot. The total kinetic energy of the robot is

$$K = \frac{1}{2}J_{11}\dot{\theta}_1^2 + \frac{1}{2}J_{22}\dot{\theta}_2^2 + J_{12}\dot{\theta}_1\dot{\theta}_2 \tag{13}$$

The gravitational potential energy of the system is given by:

$$V_g = \sum_{i=1}^{4} m_i g r_{c_{iy}} \tag{14}$$

where m_i is the mass of each component.

The elastic potential energy stored in the springs at each joint is:

$$V_p = \sum_{i=1}^{2}\frac{1}{2}k_i\left(\sqrt{a^2+b^2-2ab\cos\theta_{i,i+2}} - c_0\right)^2 \tag{15}$$

where k_i is the spring constant, a and b are the distances between the pivot points, $\theta_{i,i+2}$ is the angle between the springs, and c_0 is the natural length of the spring. The changing of angle is shown in Fig,8. The angle θ_1 decreases and the angle θ_2 increases, with both experiencing an increasing rate of change.

V. Conclusion

In summary, this study encapsulates the current state of research on jumping robots and the themes that interest researchers. It focuses particularly on jumping robots inspired by frogs and proposes several future research directions. The study derives the robot's dynamics and kinematics models and uses simulations to reveal key parameters such as friction coefficients and maximum take-off angles, offering insights into optimizing robot design to enhance mobility.

REFERENCES

[1] G. Taylor, M.S. Triantafyllou, and C. Tropea, Animal Locomotion, Des Moines, IA, USA: Springer, 2010.

[2] Mammal's Locomotion. [Online]. Available: http://mammals-locomotion.com/ [Accessed: 20-Aug-2020].

[3] X. Mo, W. Ge, M. Miraglia, F. Inglese, D. Zhao, C. Stefanini, and D. Romano, "Jumping Locomotion Strategies: From Animals to Bioinspired Robots," *Applied Sciences*, vol. 10, no. 23, p. 8607, 2020.

[4] R. Kram and T.J. Dawson, "Energetics and biomechanics of locomotion by red kangaroos (*Macropus rufus*)," *Comp. Biochem. Physiol. Part B Biochem. Mol. Biol.*, vol. 120, pp. 41–49, 1998.

[5] J. Scott, "The locust jump: An integrated laboratory investigation," *Adv. Physiol. Educ.*, vol. 29, pp. 21–26, 2005.

[6] W. Meng, X.-Z. Zang, J.-Z. Fan, and J. Zhao, "Biological jumping mechanism analysis and modeling for frog robot," *J. Bionic Eng.*, vol. 5, no. 3, pp. 181-188, 2008.

[7] D. Wei and W. Ge, "Research on one bio-inspired jumping locomotion robot for search and rescue," *Int. J. Adv. Robot. Syst.*, vol. 11, p. 168, 2014.

[8] C. Zhang, W. Zou, L. Ma, and Z. Wang, "Biologically inspired jumping robots: A comprehensive review," *Robotics and Autonomous Systems*, vol. 124, p. 103362, 2020.

[9] R. Niiyama, A. Nagakubo, and Y. Kuniyoshi, "Mowgli: a bipedal jumping and landing robot with an artificial musculoskeletal system," in *Proceedings of the IEEE International Conference on Robotics and Automation*, Roma, Italy, 2007, pp. 2546–2551.

[10] J. Burdick and P. Fiorini, "Minimalist jumping robots for celestial exploration," *Int. J. Robotics Res.*, vol. 22, pp. 653–674, 2003.

[11] G.H. Liu, H.Y. Lin, S.T. Chen, and P.C. Lin, "A bio-inspired hopping kangaroo robot with an active tail," *J. Bionic Eng.*, vol. 11, pp. 541–555, 2014.

[12] Y. Pan, J. Fan, W. Ma, F. Gao, G. Liu, and J. Zhao, "Design and motion analysis of a frog-like jumping robot based on a soft body detonation drive," *Materials & Design*, vol. 232, p. 112127, 2023.

[13] S. Wang, J. Fan, and G. Liu, "Research status and development trend of frog-inspired robots," Robotica, vol. 41, no. 7, pp. 2228-2248, 2023.

[14] J.-Z. Fan, W. Zhang, P.-C. Kong, H.-G. Cai, and G.-F. Liu, "Design and dynamic model of a frog-inspired swimming robot powered by pneumatic muscles," Chinese Journal of Mechanical Engineering, vol. 30, pp. 1123-1132, 2017.

[15] A. Igarashi and S. Mikami, "Frog-like robot with jump and walk mechanism for locomotion on rough terrain—Designing legs with biarticular muscles and slide-lock mechanism," in 2014 13th International Conference on Control Automation Robotics and Vision (ICARCV), IEEE, 2014, pp. 1788-1791.